40. Richmond, G. L. *Chem. Phys. Lett.* 110, 571–575 (1984).
41. Richmond, G. L., Rojhantalab, H. M., Robinson, J. M. & Shannon, V. L. *J. Opt. Soc. Am.* B4, 228–236 (1987).
42. Corn, R. M., Romagnoli, M., Levenson, M. D. & Philpott, M. R. *J. chem. Phys.* 81, 4127–4132 (1984).
43. Furtak, T. E., Meragliottia, J. & Korenowski, G. M. *Phys. Rev.* B 35, 2596–2572 (1987).
44. Richmond, G. L., Koos, D. A., Robinson, J. M. & Shannon, V. L., *Bull. Am. phys. Soc.* 33, 1648 (1988).
45. Shannon, V. L., Koos, D. A. & Richmond, G. L. *J. chem. Phys.* 87, 1440–1441 (1987); *Appl. Opt.* 26, 3579–3583 (1987).
46. Shannon, V. L., Koos, D. A. & Richmond, G. L. *J. phys. Chem.* 91, 5548–5555 (1987).
47. Shannon, V. L., Koos, D. A., Robinson, J. M. & Richmond, G. L. *Chem. Phys. Lett.* 142, 323–328 (1987).
48. Miragliotta, J. & Furtak, T. E. *Phys. Rev.* B 37, 1028–1030 (1988).
49. Rasing, Th., Kim, M. W., Shen, Y. R. & Grubb, S. *Phys. Rev. Lett.* 55, 2903–2906 (1985).
50. Berkovic, G., Rasing, Th. & Shen, Y. R. *J. chem. Phys.* 85, 7374–7376 (1986).
51. Bhattacharyya, K., Sitzmann, E. V. & Eisenthal, K. B. *J. chem. Phys.* 87, 1442–1443 (1987).
52. Grubb, S. G., Kim, M. W., Rasing, Th. & Shen, Y. R. *Langmuir* 4, 452–454 (1988).
53. Freund, I. & Deutsch, M. *Opt. Lett.* 11, 94–96 (1986).
54. Heinz, T. F., Chen, C. K., Ricard, D. & Shen, Y. R. *Phys. Rev. Lett.* 48, 478–481 (1983).
55. Zhu, X. Q., Suhr, H. & Shen, Y. R. *Phys. Rev.* B 35, 3047–3050 (1987).
56. Hunt, J. H., Guyot-Sionnest, P. & Shen, Y. R. *Chem. Phys. Lett.* 133, 189–192 (1987).
57. Guyot-Sionnest, P., Hunt, J. H. & Shen, Y. R. *Phys. Rev. Lett.* 59, 1597–1600 (1987).
58. Hunt, J. H., Guyot-Sionnest, P. & Shen, Y. R. in *Laser Spectroscopy VIII* (eds Persson, W. & Svanberg, S.) 253–266 (Springer, Berlin, 1987).
59. Guyot-Sionnest, P., Superfine, R. & Hunt, J. H. *Chem. Phys. Lett.* 144, 1–5 (1988).
60. Harris, A. L., Chidsey, C. E. D., Levinos, N. J. & Loiacono, D. N. *Chem. Phys. Lett.* 141, 350–356 (1987).
61. Superfine, R., Guyot-Sionnest, P., Hunt, J. H., Kao, C. T. & Shen, Y. R. *Surf. Sci.* 200, L445–L450 (1988).

ARTICLES

Designing CD4 immunoadhesins for AIDS therapy

Daniel J. Capon, Steven M. Chamow*, Joyce Mordenti†, Scot A. Marsters†, Timothy Gregory*, Hiroaki Mitsuya‡, Randal A. Byrn§, Catherine Lucas∥, Florian M. Wurm¶, Jerome E. Groopman§, Samuel Broder‡ & Douglas H. Smith

Departments of Molecular Biology, * Recovery Process Research and Development, † Medicinal and Analytical Chemistry, ¶ Cell Culture Research and Development, Genentech, Inc., 460 Point San Bruno Boulevard, South San Francisco, California, 94080, USA
‡ The Clinical Oncology Program, National Cancer Institute, National Institutes of Health, Bethesda, Maryland, 20892, USA
§ Division of Hematology-Oncology, Harvard Medical School, New England Deaconess Hospital, Boston, Massachusetts, 02215, USA

A newly-constructed antibody-like molecule containing the gp120-binding domain of the receptor for human immunodeficiency virus blocks HIV-1 infection of T cells and monocytes. Its long plasma half-life, other antibody-like properties, and potential to block all HIV isolates, make it a good candidate for therapeutic use.

DESPITE the exquisite ability of the immune system to distinguish between self and non-self, and to put forth an impressive diversity in its antigen-recognizing repertoire, it can still be outflanked by a rapidly changing pathogen. Human immunodeficiency virus type 1 (HIV-1) is an example of such a pathogen, and, as a result, its consequences are devastating. Every individual infected with the virus is expected to develop a serious or life-threatening illness[1]; no protective state has been shown to be generated in natural infections. It has not yet been possible to generate a protective response by immunizing chimpanzees with gp120, the HIV-1 envelope glycoprotein[2,3], or to confer passive immunity to chimpanzees using human IgG[4]. Even neutralizing antibodies made in experimental animals can block the infectivity of only a few HIV-1 isolates[3,5]. Thus, the prospects for eliciting protective immunity against HIV-1, or for using antibodies as therapeutic agents to control HIV-1 disease are bleak. Anti-retroviral chemotherapy using dideoxynucleosides such as AZT does help some patients, but the toxicity is such that new strategies are needed[6].

We have therefore attempted to block HIV-1 infectivity with soluble derivatives of CD4, the receptor for HIV-1, with the rationale that the CD4-binding domain of gp120 is the only part of gp120 that the virus cannot afford to change[7]. CD4 is a cell-surface glycoprotein found mostly on a subset of mature peripheral T cells that recognize antigens presented by class II MHC molecules[8,9]. Antibodies to CD4 block HIV-1 infection of T cells[10,11] and human cells not susceptible to HIV-1 infection become so after transfection with a CD4 cDNA[12]. Gp120 binds CD4 with high affinity ($K_D \sim 10^{-9}$M), suggesting that it is this interaction which is crucial to the entry of virus into cells[7,13]. Indeed, we[7] and others[14–18] have shown that soluble rCD4, lacking the transmembrane and cytoplasmic sequences of CD4, can block HIV-1 infectivity, syncytium formation, and cell killing by gp120 (ref. 19). rCD4 blocks the infectivity of diverse HIV-1 isolates (R.B., J.G., H.M. and S.B., unpublished results),

and in theory should block all. At best, however, soluble rCD4 offers only a passive defence against the virus.

Active immunity requires a molecule such as an antibody, which can specifically recognize a foreign antigen or pathogen and mobilize a defence mechanism. Antibodies comprise two functionally independent parts, a rather variable domain (Fab), which binds antigen, and an essentially constant domain (Fc), providing the link to effector functions such as complement or phagocytic cells. It is almost certainly the lack of an antigen-binding domain which can neutralize all varieties of virus that hampers the development of humoral immunity to HIV-1. We reasoned that the characteristics of CD4 would make it ideal as the binding site of an antibody against HIV-1. Such an antibody would bind and block all HIV-1 isolates, and no mutation for the virus could make, without losing its capacity to infect CD4⁺ cells specifically, would evade it. We therefore set out to construct such an antibody by fusing CD4 sequences to antibody domains.

We had two major aims for our hybrid molecules; first, as pharmacokinetic studies in several species predict that the half-life of soluble CD4 will be short in humans (30–120 min; J.M., unpublished results) we wished to construct a molecule with a longer half-life; second, we wanted to incorporate functions such as Fc receptor binding, protein A binding, complement fixation and placental transfer, all of which reside in the Fc portion of IgG. The Fc portion of immunoglobulin has a long plasma half-life, like the whole molecule, whereas that of Fab is short, and we therefore expected to be able to fuse our short-lived CD4 molecule to Fc and generate a longer-lived CD4 analogue. Because CD4 is itself part of the immunoglobulin gene superfamily, we expected that it would probably fold in a way that is compatible with the folding of Fc. We have therefore produced a number of CD4-immunoglobulin hybrid molecules, using both the light and the heavy chains of immunoglobulin, and investigated their properties. We have named one
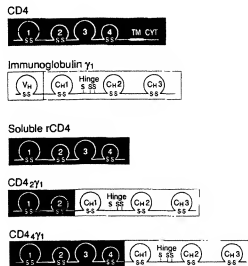
Fig. 1 Structure of cell surface CD4, human IgG1 (γ1), soluble rCD4, and CD4 immunoadhesins (2γ1 and 4γ1). The immunoglobulin-like domains of CD4 are numbered 1 to 4; TM and CYT refer to the transmembrane and cytoplasmic domains. Soluble rCD4 is truncated after proline 368 of the mature CD4 polypeptide. This results in a secreted, soluble polypeptide with an affinity for gp120 similar to that of cell surface CD4 (ref. 7). The vertical division within IgG1 indicates the junction of the variable (VH) and constant (CH1, hinge, CH2, and CH3) regions. Disulphide bonds formed within IgG1 domains and the immunoglobulin-like domains of CD4 are indicated by (S-S). The positions of cysteine residues that form intermolecular disulphide bridges connecting the IgG1 heavy-chain hinge to light and heavy chains are indicated by (S). CD4-derived and IgG1-derived domains of 2γ1 and 4γ1 are indicated by shaded and unshaded regions, respectively. The 2γ1 and 4γ1 immunoadhesins consist of residues 1 to 180 and residues 1 to 366 of the mature CD4 polypeptide, respectively, fused to the first residue (serine 114) of the human IgG1 heavy-chain constant region.

Methods. For the expression of CD4 immunoadhesins, the sequences of CD4 and human IgG1 were fused by oligonucleotide-directed deletional mutagenesis after their insertion into a mammalian expression vector used for soluble rCD4 expression[7]. A human IgG1 heavy-chain cDNA, obtained from a human spleen cDNA library using probes based on the published sequence[47], was inserted at a unique Xba1 site found immediately 3′ of the CD4 coding region in the same reading orientation as CD4. Synthetic 48-mer oligodeoxynucleotides, complementary to the 24 nucleotides at the borders of the desired CD4 and IgG1 fusion sites, were used as primers in the mutagenesis reactions using the plasmid described above as the template[48].

particularly interesting class of these CD4-immunoglobulin hybrids 'immunoadhesins', because they contain part of an adhesive molecule[20] linked to the immunoglobulin Fc effector domain.

Synthesis of CD4 immunoadhesins

CD4 is an integral membrane protein with an extracellular region comprising four domains with homology to immunoglobulin variable domains[21,22] (Fig. 1). Soluble CD4 derivatives consisting of this extracellular region bind gp120 with the same affinity as cell-surface CD4 (ref. 7). CD4 variants containing only domains 1 and 2 also bind gp120[17,18], but the affinity of this interaction is not known. We constructed a series of hybrid molecules consisting of the first two or all four immunoglobulin-like domains of CD4 fused to the constant region of antibody heavy and light chains (Fig. 1).

We investigated the synthesis and secretion of these hybrids using transient expression in a human embryonic kidney-derived cell line. As shown in Fig. 2, immunoglobulin light and heavy

chains are efficiently expressed in these cells, and light chain is efficiently secreted, but heavy chain is not unless a light chain is coexpressed. Thus the rules governing immunoglobulin chain secretion in these cells are the same as those for plasma or other lymphoid cells[25]. We first constructed hybrids that fused CD4 with the constant regions of murine κ- or γ1-chains. These hybrids contained either the first two or all four immunoglobulin-like domains of CD4, linked at a position chosen to mimic the spacing between disulphide-linked cysteines seen in immunoglobulins (Fig. 1). As expected, both κ- and γ1-chain hybrids were secreted well, whereas hybrids between CD4 and mouse γ1-chain were expressed but not secreted unless a κ-chain or a CD4-κ hybrid was present.

A different and unexpected picture emerged when analogous CD4-heavy-chain hybrids were constructed using the constant region of human IgG1 heavy chain instead of mouse heavy chain. Such hybrids, containing either the first two or all four immunoglobulin-like domains of CD4 (named 2γ1 and 4γ1 respectively), were secreted in the absence of wild-type or hybrid light chains (Fig. 2a). Both 2γ1 and 4γ1 could be directly immunoprecipitated using Staphylococcus aureus protein A, which binds the Fc portion of IgG1, indicating that the protein A-binding sites of these constructs are fully functional. Indeed, both molecules can be purified to near homogeneity on protein A columns (Fig. 2b).

Structure of CD4 immunoadhesins

We examined the subunit structure of these immunoadhesin molecules using SDS-polyacrylamide gels (Fig. 2b). Without any reducing agent, the apparent relative molecular mass (M_r) of each construct doubled, demonstrating that both immunoadhesins are disulphide-linked dimers. The hinge region of each immunoadhesin contains three cysteine residues, one normally involved in disulphide bonding to light chain, the other two in the intermolecular disulphide bonds between the two heavy chains in IgG. As the molecules are dimers at least one, and perhaps all three, of these cysteine residues are involved in intermolecular disulphide bonds. We examined the capacity of 2γ1 and 4γ1 to form disulphide links with light chains. When an immunoadhesin construct was cotransfected with a light chain, the light chain produced could be precipitated by protein A. Mutagenic substitution of the first hinge-region cysteine with alanine abolished light-chain bonding, but did not affect dimerization (data not shown), indicating that this cysteine bonds the light chain in these hybrids, as in normal IgG. Thus the disulphide bond structure of these immunoadhesins seems to be analogous to that of immunoglobulins.

gp120 binding

To determine whether our immunoadhesins retain the ability to bind gp120 with high affinity, and whether the first two immunoglobulin-like domains are sufficient, we carried out saturation binding analyses with radioiodinated gp120. Binding is saturable, showing a simple mass action curve (Fig. 3a). The dissociation constant (K_d) for the interaction of each immunoadhesin with gp120, calculated by Scatchard analysis (Fig. 3a, inset), was indistinguishable from that of soluble rCD4 (~10^{-9} M) (Table 1). Thus, the N-terminal 170 amino acids of CD4 are sufficient for high-affinity binding. As these immunoadhesins are homodimeric, they should each have two gp120-binding sites. We examined this possibility by coating plastic microtitre wells with gp120, then adding soluble CD4 or immunoadhesins. Both immunoadhesins could bind added labelled gp120, whereas soluble rCD4, with only one gp120 binding site, could not (J. Porter and S. C., unpublished results). To confirm the bivalent nature of 2γ1 and 4γ1, we examined their ability to agglutinate sheep red blood cells coated with gp120. Again, both CD4 immunoadhesins, but not soluble rCD4, agglutinated the cells, showing that binding to gp120 molecules on different cells is not sterically hindered.
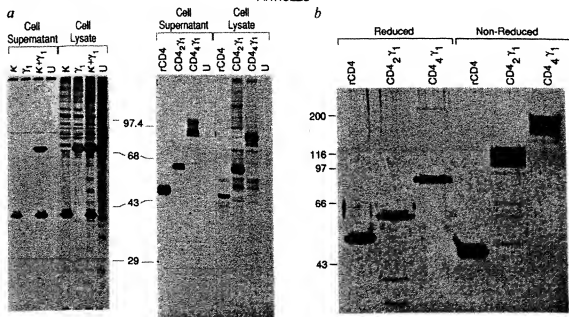
Fig. 2 Expression, secretion and subunit structure of CD4 immunoadhesins and soluble rCD4. *a*, Expression and secretion of mouse immunoglobulins, soluble rCD4 and CD4 immunoadhesins expressed in mammalian cells. Cells were transfected with vectors directing the expression of murine κ-light chain (lanes κ) or γ1-heavy chain (lanes γ1) individually or together (lanes κ + γ1), vectors encoding soluble rCD4 (lanes rCD4), and the CD4 immunoadhesins 2γ1 (lanes CD4,2γ1) or 4γ1 (lanes CD4,γ1). After metabolic labelling with [35S]methionine, cell supernatants and cell lysates were analysed by immunoprecipitation. Lanes U, untransfected cells. *b*, Subunit structure of secreted CD4 immunoadhesins and soluble rCD4. Soluble rCD4, 2γ1 and 4γ1 were purified from culture supernatants of transfected cells and analysed by electrophoresis on a 7.5% SDS-polyacrylamide gel. Samples were prepared in buffer with 10 mM dithiothreitol (DTT) (reducing conditions) or without DTT (non-reducing conditions). The positions of relative molecular mass standards are indicated (in thousands). Both immunoadhesins behaved as disulphide-linked dimers; in contrast, soluble rCD4 which is monomeric, displayed only a minor change in mobility upon reduction of its intra-molecular disulphide bonds.
Methods. *a*, Cells were transfected by a modification of the calcium phosphate procedure, labelled with [35S]methionine, and cell lysates prepared as described[?]. Immunoprecipitation analysis was carried out as previously described[7], with the exception that no preadsorbtion with Pansorbin (Calbiochem) was done, and the precipitating antibodies used were 2 μl of rabbit anti-mouse IgG serum (Cappell) for mouse IgG heavy and light chains, 0.25 μg of OKT4A (Ortho) for soluble rCD4, and no added antibody (Pansorbin only) for the CD4 immunoadhesins. Immunoprecipitated proteins were resolved on 10% SDS-PAGE gels, and visualized by autoradiography. *b*, CD4 immunoadhesins were purified from transfected cell supernatants by protein A affinity chromatography followed by ammonium sulphate precipitation. Purified proteins were subjected to SDS-PAGE under both reducing and non-reducing conditions and visualized by silver staining.

In vivo plasma half-life

We examined whether the immunoadhesins share the long *in vivo* half-life of antibodies. Studies of rCD4 in rabbits provide clearance data that extrapolate well to other species, including humans (J.M., unpublished results). The change in plasma concentration with time for each of the three CD4 analogues in rabbits is shown in Fig. 4. Analysis of these data reveals that soluble rCD4 has a terminal half-life in rabbits of ~15 min, whereas 4γ1 and 2γ1 have terminal half-lives of ~7 and 48 h, respectively (Table 1). Thus the half-life of 2γ1 in rabbits is nearly 200 times longer than that of rCD4 and comparable to that of human IgG in rabbits (4.7 days)[24]. The half-life of 2γ1 in humans is expected to be longer than that in rabbits, because of the decreased proportional blood flow to eliminating organs

as species increase in size[25], and should be comparable with that of human IgG (21 days).

Our results confirm our initial hypothesis that, as in the case of immunoglobulin itself, one can increase the stability of a rapidly cleared molecule (Fab or rCD4) by fusing it to a long-lived molecule, Fc. The swift clearance of rCD4 is probably largely due to its size, Mr 55,000, which means it is just small enough to be cleared efficiently by renal filtration. One component in the increased half-lives of these molecules is therefore probably their larger size; but this cannot be the whole story as 4γ1, although larger than 2γ1, has a shorter half-life. Both 4γ1 and rCD4, but not 2γ1, contain two CD4-derived Asn-linked carbohydrate sites which are glycosylated in rCD4 (R. Harris and M. Spellman, unpublished results); these sugar moieties

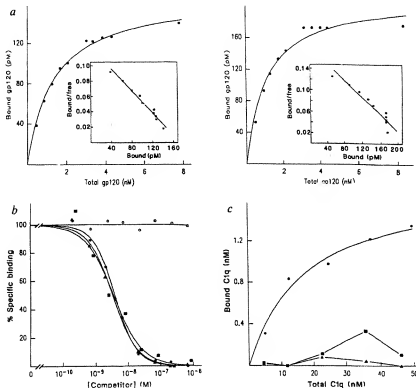**Table 1** Properties of CD4 immunoadhesins and soluble rCD4

	Calculated Mr	Subunit structure	gp120 binding (nM)*	Blocks infectivity T cells	MØ	Plasma half-life in rabbits (hours)†	Fc binding (nM)*	Complement binding	Protein A binding
rCD4	41,000	monomer	2.3 ± 0.4	Yes	Yes	0.25 ± 0.01	—	No	No
4γ1	154,000	dimer	1.2 ± 0.1	Yes	Yes	6.7 ± 1.1	2.3 ± 0.7	No	Yes
2γ1	112,000	dimer	1.4 ± 0.1	Yes	Yes	48.0 ± 8.6	2.6 ± 0.3	No	Yes
IgG1	146,000	tetramer (H₂L₂)	—	—	—	113‡	3.2 ± 0.2	Yes	Yes

* Standard error of the mean was determined using the Inplot and Scatplot programs (see Fig. 3 legend). † Standard deviation indicated in hours.
‡ Determined in ref. 24 (IgG1 has a half-life of 21 days in humans).

Fig. 3 Binding properties of CD4 immuno-
adhesins. a, Gp120 saturation binding analysis
of CD4 immunoadhesins. Immunoadhesin pro-
teins 4γ1 (left) or 2γ1 (right) in transfected cell
supernatants were incubated with increasing
concentrations of purified soluble rgp120 (ref.
50) radioiodinated with lactoperoxidase. The
lines drawn for the binding curves and for the
Scatchard plots of the data (shown in the insets)
represent the best fit as determined by unweigh-
ted least-squares linear regression analysis. Dis-
sociation constants calculated from these
results and from binding studies of gp120 to
soluble rCD4 performed in parallel are given
in Table 1. b, Binding of CD4 immunoadhesins
to Fcγ receptors on U937 cells. Competition
binding analysis was carried out by mixing
0.1 μg ml⁻¹ of ¹²⁵I-labelled human IgG1 (Cal-
biochem) with increasing concentrations of
purified human IgG1 (solid circle), 2γ1 (solid
square), 4γ1 (solid triangle), or soluble rCD4
(open circle) proteins. Curves drawn represent
the best fit as determined by unweighted least-
squares nonlinear (IgG1, 2γ1 and 4γ1) or linear
(rCD4) regression analysis. Dissociation con-
stants calculated from these results are shown
in Table 1. c, Clq saturation binding analysis
of CD4 immunoadhesins. Purified anti-gp120
IgG2a mouse monoclonal antibody (solid
circle), 2γ1 (solid square), or 4γ1 (solid
triangle) proteins were aggregated by binding
to gp120-coupled Sepharose, and incubated
with increasing concentrations of purified
human C1q (Calbiochem) radioiodinated with
lactoperoxidase. The curve drawn for the anti-gp120 monoclonal antibody (mAb) represents the best fit as determined by least-squares nonlinear
regression analysis; the dissociation constant for C1q binding to this gp120-aggregated anti-gp120 mAbs was ~1.8×10⁻⁸ M.
Methods. a, Gp120 saturation binding analysis was carried out as described⁷ except that gp120-CD4 immunoadhesin complexes were collected
directly onto Pansorbin: binding was comparable to that observed when complexes were collected with OKT4A as for soluble rCD4. Specifically
bound ¹²⁵I-labelled gp120 was determined from the difference in binding in the presence or absence of a 1,000-fold excess of unlabelled
rgp120 and is plotted against the solid ¹²⁵I-labelled gp120 concentration. b, FcR binding analysis was done essentially as described²⁷ except
that after centrifugation free IgG1 was removed by aspiration of the aqueous and oil layers. Mixtures of ¹²⁵I-labelled human IgG1 and IgG1,
CD4 immunoadhesins or soluble rCD4 were incubated with U937 cells (2×10⁶ cells per tube) for 60 min at 4 °C. Specific binding was calculated
by subtracting residual nonspecific binding (<25% of specific binding) which could not be competed out by a 1,000-fold excess of unlabelled
human IgG1. c, C1q binding analysis was done essentially as described²⁹, except that gp120 coupled to CNBr-activated Sepharose 6B (Pharmacia)
was used as the solid support to aggregate CD4 immunoadhesins or the anti-gp120 mouse mAb. Proteins were adsorbed to gp120 coupled-beads,
incubated with varying concentrations of ¹²⁵I-labelled C1q, and bound and free C1q were then separated by centrifugation through 20%
sucrose. Specific binding was determined from the difference in binding in the presence or absence of added antibody or immunoadhesin. All
data analysis was carried out using the Inplot and Scatplot programs (R. Vandlen, Genentech). Scatplot was modified from the Ligand program
(P. Muncy, NIH).

may facilitate clearance by receptors in the liver. The charge of
the molecule may also be important, as the CD4 portion of 4γ1
contributes a net excess of eleven positively charged amino acids
on 4γ1, but only three on 2γ1. This may increase uptake of
rCD4 and 4γ1 onto anionic surfaces, accelerating their clearance
from the circulation.

Fc receptor and complement binding

Two major mechanisms for the elimination of pathogens are
mediated by the Fc portion of specific antibodies. Fc activates
the classical pathway of complement, ultimately resulting in
lysis of the pathogen, whereas binding to cell Fc receptors can
lead to ingestion of the pathogen by phagocytes or lysis by killer
cells. The binding sites for Fc cell receptors and for the initiating
factor of the classical complement pathway, C1q, are found in
the constant region of heavy chain²⁶ (the CH2 domain for C1q²⁷
and the region linking the hinge to CH2 for Fc cell receptors²⁸).
We aimed to incorporate both of these functions into the
immunoadhesins. We chose the IgG1 subtype to supply the Fc
domain because IgG1 is the best compromise between Fc bind-
ing, C1q binding, and long half-life. We show below that the
immunoadhesins bind FcR well, but do not bind C1q.

Three types of Fc cell receptors are known to be expressed
on a variety of leukocytes. Of these FcRI, principally expressed

on mononuclear phagocytes, is the only one which binds
monomeric human IgG1 with high affinity²⁶. We used competi-
tion binding analysis with FcRI receptors on the U937
monocyte/macrophage cell line to characterize the Fc receptor
binding of 2γ1 and 4γ1. Direct saturation binding analysis with
human IgG1 gave a K_d of ~3×10⁻⁹ M. In competition bind-
ing analyses, the two CD4 immunoadhesins, but not rCD4,
bound to Fc receptors on U937 cells to the same extent and
with an affinity indistinguishable from human IgG1 (Fig. 3b,
Table 1).

We examined the ability of the immunoadhesins to bind to
the first component of the classical pathway of complement,
C1q, by saturation binding analysis. Because binding of C1q
increases with the aggregation state of the antibody, with an
affinity of ~10⁻⁴ for monomers and ~10⁻⁸ for tetramers of
IgG²⁶, we first aggregated the immunoadhesin using gp120
linked to Sepharose. As a positive control, we measured C1q
binding to an anti-gp120 mouse IgG2a monoclonal antibody,
(which like human IgG1 binds C1q with high affinity²⁹) aggre-
gated by the same gp120-Sepharose. The affinity of the mouse
antibody for C1q determined by Scatchard analysis was 1.8×
10⁻⁸ M (Fig. 3c), comparable to that observed for other mouse
IgG2a and for human IgG1 antibodies. In contrast, neither
immunoadhesin bound C1q to any detectable extent (Fig. 3c),

Fig. 4 Pharmacokinetics of CD4 immunoadhesins and soluble rCD4. Shown are the mean plasma concentrations (ng ml^{-1}) for 2γ1 (triangles), 4γ1 (squares), and rCD4 (circles) following a single intravenous administration in rabbits. a, Time course of plasma clearance over the first 120 minutes; b, time course over 8 days after injection of the CD4 analogues. **Methods.** Ten female New Zealand white rabbits (Rabbitek, Modesto, California) were injected intravenously (via an ear vein catheter) with a single bolus dose (40 μg kg^{-1} in a volume of 1 ml) of either rCD4 ($n = 2$), 4γ1 ($n = 4$), or 2γ1 ($n = 3$). Blood samples were obtained from an arterial catheter in the opposite ear; after 24 hours, blood samples were obtained by venipuncture. Plasma concentrations of each protein were determined by an enzyme-linked immunosorbent assay. This capture assay used two antibodies, including an anti-CD4 monoclonal directed against the gp120-binding site (and capable of blocking gp120 binding), and thus provided a sensitive assay for CD4-containing molecules that are still capable of binding gp120. Exponential equations were fitted to the data of individual rabbits using a nonlinear least squares regression program NONLIN84[40] (Statistical Consultants, Lexington, Kentucky). The concentration (C, ng ml^{-1}) versus time (t) data for rCD4 were best described by a biexponential equation $C = 661 \text{ e}^{-1.34t} + 620 \text{ e}^{-0.0472t}$ where time is in minutes; the average terminal half-life was 14.7 min, and the average clearance was 3 ml min^{-1} kg^{-1}. The 4γ1 data were best described by a triexponential equation, $C = 546 \text{ e}^{-211t} + 193 \text{ e}^{-20.5t} + 46.8 \text{ e}^{-2.54t}$, where time is in hours. The average terminal half-life was 6.7 hours, and the average clearance was 0.91 ml min^{-1} kg^{-1}. The 2γ1 data were best described by a triexponential equation, $C = 153 \text{ e}^{-53.2t} + 342 \text{ e}^{-2.19t} + 183 \text{ e}^{-0.331t}$, where time is in hours. The average terminal half-life was 48 hours, and the average clearance was 0.039 ml min^{-1} kg^{-1}.
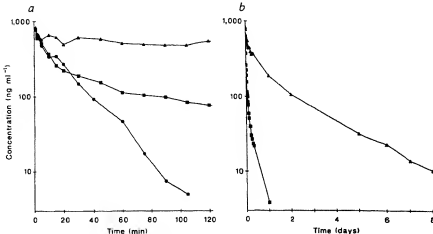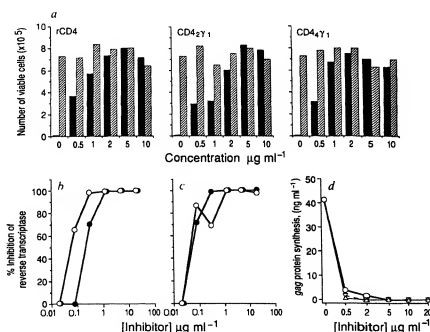

Fig. 5 Inhibition of HIV-1 infectivity by CD4 immunoadhesins and soluble rCD4. a, Inhibition of the cytopathic effects on ATH8 cells by HIV-1 was examined as described[31] with the HTLV-IIIB isolate[31]. The number of viable cells at day 10 after infection is shown for varying concentrations of each molecule in the presence (solid bars) or absence (shaded bars) of added virus. The absence of an effect of each CD4 analogue on cell number in the absence of virus indicates that none of these molecules inhibited cell growth. b, Inhibition of infection of H9 cells by HIV-1 was carried out as described[7] with the HTLV-IIIB isolate. Reverse transcription activity was determined 7 days after infection and is given as the percentage of the level seen in the absence of inhibitor. Solid and open circles represent 2γ1 and 4γ1, respectively. c, Inhibition of infection of U937 cells by HIV-1 (HTLV-IIIB isolate) was carried out as described above for H9 cells. d, Inhibition of infection of fresh human monocytes by the monocytotropic HIV-1 isolate Ba-L (ref. 35). HIV-1 replication was determined by measuring the level of p24 gag antigen synthesis 10 days after infection using a commercial assay kit (Dupont). Circles, inverted triangles and triangles represent inhibition of p24 synthesis by soluble rCD4, 2γ1 and 4γ1, respectively.

although both did bind the gp120-Sepharose matrix in amounts comparable to the control antibody.

Thus, our immunoadhesins bind well to Fc receptors. It is perhaps surprising that they do not bind C1q. As far as is known, all the critical contact residues for C1q binding reside in the CH2 domain of the heavy chain[26], and are conserved among all the human IgG isotypes. However, these have varying abilities to mediate complement fixation. Thus steric hindrance or other aspects of protein conformation (for example, the segmental flexibility of antibodies[30]) may be important.

Infectivity studies

Two systems were used to study the *in vitro* ability of CD4 immunoadhesins and soluble rCD4 to block infection of CD4-bearing T cells by the HIV-1 T-lymphotrophic isolate HTLV-IIIB (ref. 31). Infection with HIV-1 exerts a profound cytopathic effect on the human T-cell clone ATH8, with more than 98% of the cells being killed by day 10 after infection[32] (Fig. 5a). Both CD4 immunoadhesins blocked cell killing with the same potency as soluble rCD4, without inhibiting cell proliferation; each CD4 analogue completely abolished cell killing at a concentration of ~0.05 μM (Fig. 5a). Complete protection was also observed at comparable concentrations with a different HIV-1 isolate, HTLV-III RF, which is not neutralized by sera from animals immunized with rgp120 from the IIIB isolate[5]. We also examined the production of HIV-1 reverse transcriptase activity after infection of the H9 human T-cell line. Again, both immunoadhesins completely blocked virus production by day 7 (Fig. 5b), at

concentrations comparable to rCD4 (data not shown); moreover the potency of each CD4 analogue was markedly higher (~fivefold) than that observed in the ATH8 assay.

Monocyte infection

Because it has been suggested that antibodies present in sera from HIV-1 infected individuals may enhance the infectivity of HIV-1 in Fc receptor (FcR)-bearing cells such as primary blood monocytes[33], and monocyte cell lines[34], we examined the effect of rCD4 and CD4 immunoadhesins on HIV-1 infection of FcR-expressing cells of monocyte/macrophage origin. Both CD4 immunoadhesins completely blocked HIV-1 IIIB virus production in U937 cells at similar concentrations to those found to be effective on H9 cells (Fig. 5c), with a potency comparable to that of soluble rCD4 (data not shown). In another system, the replication of a monocytotrophic HIV-1 isolate, Ba-L[35], in fresh monocytes was monitored by the production of p24 antigen. Soluble rCD4 completely blocked infection, indicating that infection of monocytes by the Ba-L isolate does involve CD4. Both CD4 immunoadhesins also completely blocked p24 production, at concentrations equal to or lower than rCD4 (Fig. 5d). Thus the CD4 immunoadhesins are at least comparable to soluble rCD4 in their ability to prevent infection of monocyte/macrophages by HIV; no evidence was found for enhancement of infection by immunoadhesins (or by soluble rCD4) in cells which express high affinity Fc receptors.

Implications for treatment of HIV-1 disease

Because the hallmark of HIV-1 disease is the specific destruction of CD4+ T cells, and the progression of infected individuals to AIDS closely parallels their decline in CD4+ T-cell number[36], it is reasonable to believe that the interaction of gp120 with CD4, either by direct HIV-1 infection of CD4+ cells or otherwise, underlies the killing of CD4+ cells. Therefore, if this interaction can be stopped it may be possible to prevent disease progression. But despite the logic of this hypothesis, the observation that only a very few lymphocytes are actively infected with HIV-1 in vivo[37] has posed a problem to those attempting to explain the causative role of HIV-1 in the aetiology of AIDS[38]. Two observations may explain the 'catalytic' ability of HIV-1 to deplete CD4+ lymphocytes: first, a single infected cell can fuse many uninfected CD4+ cells to itself, creating an inviable mass[39,40]; and second, gp120 is shed from the surface of HIV-1-infected cells and virions[41], as its link to gp41, its anchor protein partner, is probably non-covalent. This shed gp120 binds to surface CD4 on uninfected cells with high affinity, and can result in their functional alteration[42,43] or death by one of two pathways shown to operate in vitro. Bystander cells coated with gp120 bound to their CD4 surface molecules become targets for anti-gp120 antibodies produced by HIV-1 infected individuals and can be killed via antibody-dependent cell-mediated cytotoxicity[44]. Also, MHC class II-positive CD4+ T cells can internalize gp120 bound tightly to CD4 on their surface, process it, and present peptides derived from it on their class II molecules, thus becoming sensitive, even at low gp120 concentrations, to lysis by gp120-specific cytotoxic T cells[19,45,46]. The important common factor in all these proposed mechanisms of cell destruction is that gp120 must bind specifically to cell-surface CD4. If these mechanisms are important in vivo, this would imply that soluble rCD4 could intervene.

But to affect the disease noticeably, one would expect to need to maintain a high concentration of rCD4, which is hampered by its rapid clearance. Our approach to this problem was to fuse the gp120-binding domain of CD4 to a molecule well designed to avoid the clearance mechanisms of the body. Indeed, the Fc domain and CD4 sequences are structurally compatible, as the hybrid molecules have important properties of both parents. Thus, they bind gp120 and block infection of T cells by T-lymphotrophic HIV-1 and of monocytes by mono-cytotrophic HIV-1. They are also comparable to antibodies in

their long plasma half-life and their ability to bind Fc receptors and protein A. This combination of properties allows both a better passive defence, due to the higher plasma concentrations attainable even with infrequent injection, and the possibility of actively attacking HIV-1 and infected cells. A high steady-state level also makes it more likely that effective concentrations will be attained in lymph and lymphatic organs, where HIV may be most active.

The high-affinity binding of the immunoadhesins to Fc receptors implies that mechanisms of pathogen elimination, such as phagocytic engulfment and killing by antibody-dependent cell-mediated cytotoxicity, may be recruited by these immuno-adhesins to kill HIV-1 infected cells and virus. As it is possible that antibody-dependent cell-mediated cytotoxicity in an infected individual may be more a mechanism of pathology in HIV-1 infection than a protective response[44], it is important to note a difference between CD4 immunoadhesins and the patients' own anti-gp120 antibodies: the immunoadhesin, in contrast to anti-body, cannot recognize gp120 bound to an uninfected CD4+ bystander cell, as gp120 has only a single binding site for CD4. Because placental transfer of antibody, unique to the IgG sub-class, also proceeds through an FcR-dependent mechanism, CD4 immunoadhesins may also be transferred in utero. This may have implications for the prevention of perinatally transmitted HIV-1 infection.

Although it is not yet clear which of the functions of immunoglobulins will be advantageous when applied to HIV infection, we have taken the approach of trying to add all possible functions to our immunoadhesins. Once the structural requirements for the optimal molecule are established, functions can be tailored at will, as the parent antibody molecule is so well understood.

We thank Drs Paula Jardieu, Avi Ashkenazi and Stephen Sherwin for advice and helpful discussions, Dr Rebecca Ward for helpful discussions and critical reading of the manuscript, Steven Fire for performing CD4 enzyme-linked immunosorbent assays, Vivek Bajaj and Wally Tanaka for large scale cell culture, Drs R. Harris, M. Spellman and J. Porter for allowing us to cite unpublished data, Steve Williams for murine immunoglobulin cDNAs, Mark Vasser, Parkash Jhurani and Peter Ng for synthetic DNA, Dr Brian Fendly and Kim Rosenthal for anti-gp120 monoclonals, and Carol Morita and Kerrie Andow for preparation of the figures. R.B. and J.G. are supported by grants from the NIH and the US Defense Department.

1. Curran, J. et al. Science 239, 610–616 (1988).
2. Hu, S.-L. et al. Nature 328, 721–723 (1987).
3. Berman, P. et al. Proc. natn. Acad. Sci. U.S.A. 85, 5200–5204 (1988).
4. Prince, A. et al. Proc. natn. Acad. Sci. U.S.A. 85, 6944–6948 (1988).
5. Weiss, R. et al. Nature 324, 572–575 (1986).
6. Mitsuya, H. & Broder, S. Nature 325, 773–778 (1987).
7. Smith, O. et al. Science 238, 1704–1707 (1987).
8. Sattentau, Q. & Weiss, R. Cell 52, 631–633 (1988).
9. Janeway, C. Nature 335, 208–210 (1988).
10. Dalgleish, A. et al. Nature 312, 763–767 (1984).
11. Klatzmann, D. et al. Nature 312, 767–768 (1984).
12. Maddon, P. et al. Cell 47, 333–348 (1986).
13. McDougal, J. et al. Science 231, 382–385 (1986).
14. Fisher, R. et al. Nature 331, 76–78 (1988).
15. Hussey, R. et al. Nature 331, 78–81 (1988).
16. Deen, K. et al. Nature 331, 82–84 (1988).
17. Traunecker, A., Luke, W. & Karjalainen, K. Nature 331, 84–86 (1988).
18. Berger, E., Fuerst, T. & Moss, B. Proc. natn. Acad. Sci. U.S.A. 85, 2357–2361 (1988).
19. Siliciano, R. et al. Cell 54, 561–575 (1988).
20. Doyle, C. & Strominger, J. Nature 330, 256–259 (1987).
21. Maddon, P. et al. Cell 42, 93–104 (1985).
22. Clark, S., Jefferies, W., Barclay, A., Gagnon, J. & Williams, A. Proc. natn. Acad. Sci. U.S.A. 84, 1649–1653 (1987).
23. Dorai, H. & Moore, G. J. Immun. 139, 4232–4241 (1987).
24. Nakamura, R., Spriggelberg, H., Lee, S. & Wiegle, W. J. Immun. 100, 376–383 (1968).
25. Mordenti, J. J. Pharmacol. Sci. 75, 1028–1040 (1986).
26. Burton, O. Molec. Immun. 22, 161–206 (1985).
27. Duncan, A. & Winter, G. Nature 332, 738–740 (1988).
28. Duncan, A., Woof, J., Partridge, L., Burton, D. & Winter, G. Nature 332, 563–564 (1988).
29. Leatherbarrow, R. & Dwek, R. Molec. Immun. 21, 321–327 (1984).
30. Feinstein, A., Richardson, N. & Taussig, M. J. Immun. Today 7, 169–174 (1986).
31. Gallo, R. et al. Science 224, 500–505 (1984).
32. Mitsuya, H. & Broder, S. Proc. natn. Acad. Sci. U.S.A. 83, 1911–1915 (1986).

53. Homsy, J., Tateno, M. & Levy, J. *Lancet* i, 1285–1286 (1988).
54. Takeda, A., Tuazon, C. & Ennis, F. *Science* 242, 580–583 (1988).
55. Gartner, S. *et al. Science* 233, 215–219 (1986).
56. Lane, H. & Fauci, A. *A. Rev. Immun.* 3, 477–500 (1985).
57. Harper, M., Marselle, L., Gallo, R. & Wong-Staal, F. *Proc. natn. Acad. Sci. U.S.A.* 83, 772–776 (1986).
58. Duenberg, P. *Science* 241, 514 (1988).
59. Lifson, J., Reyes, G., McGrath, M., Stein, B. & Engelman, E. *Science* 232, 1123–1127 (1986).
40. Sodroski, J., Goh, W., Rosen, C., Campbell, K. & Haseltine, W. *Nature* 322, 470–474 (1986).
41. Schneider, I., Kaaden, O., Copeland, T. D., Oroslan, S. & Hunsmann, G. *J. gen Virol.* 67, 2533–2539 (1986).

42. Lynette, G., Hartzman, R., Ledbetter, J. & June, C. *Science* 241, 573–576 (1988).
43. Kornfeld, H., Cruikshank, W., Pyle, S., Berman, J. & Center, D. *Nature* 335, 445–448 (1988).
44. Lyerly, H. Matthews, T., Langlois, A., Bolognesi, D. & Weinhold, K. *Proc. natn. Acad. Sci. U.S.A.* 84, 4601–4605 (1987).
45. Lanzavecchia, A., Roosneck, E., Gregory, T., Berman, P. & Abrignani, S. *Nature* 334, 530–532 (1988).
46. Sethi, K., Naher, H. & Stroehmann, I. *Nature* 335, 178–181 (1988).
47. Zilinan, P. J., Benson, B. J. & Hood, L. E. *Nucleic Acids Res.* 10, 4071–4079 (1982).
48. Zoller, M. & Smith, M. *Nucleic Acids Res.* 10, 6487–6500 (1982).
49. Muesing, M., Smith, D. & Capon, D. *Cell* 48, 691–701 (1987).
50. Lasky, L. *et al. Cell* 50, 975–985 (1987).

LETTERS TO NATURE

A 110-ms pulsar, with negative period derivative, in the globular cluster M15

A. Wolszczan*, S. R. Kulkarni†, J. Middleditch‡,
D. C. Backer§, A. S. Fruchter‖ & R. J. Dewey¶#

* Arecibo Observatory, Arecibo, Puerto Rico 00613
† Department of Astronomy, California Institute of Technology, Pasadena, California 91125, USA
‡ Computing and Communications Division, Los Alamos National Laboratory, Los Alamos NM 87545, USA
§ Astronomy Department, University of California, Berkeley, California 94720, USA
‖ Joseph Henry Laboratories and Physics Department, Princeton University, Princeton, New Jersey 08544, USA
¶ Center for Radiophysics and Space Research, Cornell University, Ithaca, New York, 14853, USA

We report the discovery of a 110-ms pulsar, PSR2127 + 11, in the globular cluster M15 (NGC7078)[1]. The results of nine months of timing measurements place the new pulsar about 2″ from the centre of the cluster, and indicate that it is not a member of a close binary system. The measured negative value of the period derivative, $\dot{P} \approx -2 \times 10^{-17}$ s s^{-1}, is probably the result of the pulsar being bodily accelerated in our direction by the gravitational field of the collapsed core of M15. This apparently overwhelms a positive contribution to $\dot{P}$ due to magnetic braking. Although PSR2127 + 11 has an unexpectedly long period, we argue that it belongs to the class of 'recycled' pulsars, which have been spun up by accretion in a binary system. The subsequent loss of the pulsar's companion is probably due to disruption of the system by close encounters with other stars[2,3].

The discoveries of millisecond pulsars in globular clusters M28 (ref. 4) and M4 (ref. 5) led us to survey all clusters accessible to the 305-m Arecibo radio telescope ($0° \leqslant \delta \leqslant 38°$). A dual-polarization, 40-MHz-bandwidth signal at 1415 MHz was passed through the Arecibo digital correlator, sampled with 128 lags every 506.6 μs, and recorded on tape. The relatively high central radio frequency ensured an almost interference free signal and minimized the effects of interstellar dispersion and scattering, which can be significant for distant, low-galactic-latitude clusters. M15 was observed on 28 December 1987 for 90 minutes, which corresponds to ~11 million samples.

The data were analysed at both the Cornell National Supercomputer Facility (IBM 3090-600E) and the Los Alamos National Laboratory (Cray X-MP). Both analyses involved preliminary dedispersion of the multichannel data at 128 or 64 trial dispersion measures, followed first by one-dimensional Fourier transformation of the dedispersed time series and then by a search for harmonically related spikes in the resultant power spectra. The Cray X-MP analysis used the full, 11-million-sample data arrays to obtain maximum sensitivity with regard to isolated pulsars. The data analysed with the IBM supercom-
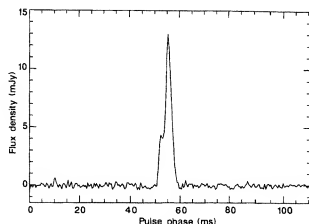
Fig. 1 The average pulse profile of PSR2127 + 11 at 1415 MHz. The effective resolution is ~800 μs and the integration time is 7 hours.

puter were divided into five 2-million-sample blocks, which were treated separately to maintain high sensitivity to binary pulsars with short orbital periods. The nominal 6σ sensitivities of these two analysis schemes were 0.05 mJy and 0.1 mJy respectively, for the periods down to ~2.5 ms.

The data analysis at Cornell revealed the presence of a 110-ms, high-Q periodicity in the received signal with dispersion measure DM ≈ 60 pc cm^{-3}. This detection was subsequently confirmed at Los Alamos. Further observations made at Arecibo on 20 and 21 February 1988 confirmed the discovery of a 110-ms pulsar. The average pulse profile of PSR2127 + 11 observed at 1415 MHz is shown in Fig. 1. The pulsar parameters, derived from our twice-weekly timing observations over nine months, are summarized in Table 1. Errors quoted are the standard 3σ errors of a model fit to the observed pulse arrival times.

Although the precise timing and Very Large Array (VLA) positions of PSR2127 + 11 will become known soon, the present positional accuracy is sufficient to conclude that the pulsar is located well within the 6″ core radius of the cluster, 2.0″ west and 0.6″ north of the centre[6]. The dispersion measure of PSR2127 + 11, DM = 67.25 pc cm^{-3}, agrees well with that expected from a simple model of the galactic electron density distribution[7], given the distance, $D = 9.7$ kpc, and galactic coordinates,

Table 1 Measured parameters of the pulsar PSR2127 + 11

Pulsar period	0.11066470954 ± 0.00000000001 s
Period derivative	$(-20 \pm 1) \times 10^{-18}$ s s^{-1}
Epoch	JD 2447213.15
Dispersion measure	67.25 ± 0.05 pc cm^{-3}
Flux density (430 MHz)	1.7 ± 0.4 mJy
Flux density (1400 MHz)	0.2 ± 0.05 mJy
Right Ascension (B1950.0)	$21^h27^m33.22^s \pm 0.01$
Declination (B1950.0)	$11°56'49.4'' \pm 0.3$
Distance	9.7 kpc